6-19-2018

Crop Residue Burning in Northern India: Increasing Threat to Greater India

S. Sarkar
NASA Goddard Space Flight Center

Ramesh P. Singh
Chapman University, rsingh@chapman.edu

A. Chauhan
Sharda University

Recommended Citation

Sarkar, S., Singh, R. P., & Chauhan, A. (2018). Crop residue burning in northern India: Increasing threat to Greater India. *Journal of Geophysical Research: Atmospheres*, 123. https://doi.org/10.1029/2018JD028428

Crop Residue Burning in Northern India: Increasing Threat to Greater India

Comments

This article was originally published in *Journal of Geophysical Research: Atmospheres*, volume 123, in 2018. DOI: 10.1029/2018JD028428

Copyright

Journal of Geophysical Research: Atmospheres

RESEARCH ARTICLE
10.1029/2018JD028428

Crop Residue Burning in Northern India: Increasing Threat to Greater India

S. Sarkar[1,2], R. P. Singh[3], and A. Chauhan[4]

[1]NASA Goddard Space Flight Center, Greenbelt, MD, USA, [2]Science Systems and Applications, Inc., Lanham, MD, USA, [3]School of Life and Environmental Sciences, Schmid College of Science and Technology, Chapman University, Orange, CA, USA, [4]School of Engineering and Technology, Sharda University, Greater Noida, India

Key Points:
- Analysis from multiple sources proves the greater influence of crop residue burning over rest of India
- This paper shows an increasing effect of crop residue burning over central and eastern India
- We demonstrate an increasing impact since the year 2010 with an increase in mechanized harvesting practice

Supporting Information:
- Figure S1
- Supporting Information S1

Correspondence to:
S. Sarkar,
sudipta.sarkar@nasa.gov

Citation:
Sarkar, S., Singh, R. P., & Chauhan, A. (2018). Crop residue burning in northern India: Increasing threat to Greater India. *Journal of Geophysical Research: Atmospheres*, *123*. https://doi.org/10.1029/2018JD028428

Received 29 JAN 2018
Accepted 2 JUN 2018
Accepted article online 19 JUN 2018

Abstract Crop residue burning (CRB) is a recurring problem, during October–November, in the northwestern regions (Punjab, Haryana, and western Uttar Pradesh) of India. The emissions from the CRB source regions spread in all directions through long-range transport mechanisms, depending upon the meteorological conditions. In recent years, numerous studies have been carried out dealing with the impact of CRB on the air quality of Delhi and surrounding areas, especially in the Indo-Gangetic Basin (also referred to as Indo-Gangetic Plain). In this paper, we present detailed analysis using both satellite- and ground-based sources, which show an increasing impact of CRB over the eastern parts of the Indo-Gangetic Basin and also over parts of central and southern India. The increasing trends of finer black carbon particles and greenhouse gases have accelerated since the year 2010 onward, which is confirmed by the observation of different wavelength dependent aerosol properties. Our study shows an increased risk to ambient air quality and an increased spatiotemporal extent of pollutants in recent years, from CRB, which could be a severe health threat to the population of these regions.

Plain Language Summary This paper shows from multiple evidence increasing effects of crop residue burning on the rest of India. This is the first work of its kind that treats this issue over rest of India at depth based on data from multiple sources and shows the ever increasing menace of biomass burning to air pollution.

1. Introduction

Air pollution in Indian subcontinent has been identified as a critical issue that is having a lasting impact on public health and mortality rates (Ghude et al., 2016; Gurjar et al., 2010; Laumbach & Kipen, 2012; Simon et al., 1998; World Health Organization, 2016). Long-term studies, carried out across different Indian cities, have all reported persistently high values of aerosol (Girolamo et al., 2004; Moorthy et al., 2013; Prasad et al., 2006; Sarkar et al., 2006; Satheesh et al., 2017), PM2.5 and PM10 (Guttikunda & Jawahar, 2012; Sharma et al., 2003; Sharma & Maloo, 2005), and NO_x (Badhwar et al., 2006; Ghude et al., 2008). Ascertaining the exact source of air pollution in India is complicated by several factors. This includes the intermixing of pollutants derived from local origin and long-range transport mechanisms (Badarinath et al., 2009; Kumar et al., 2015), increase in vehicular traffic (Pucher et al., 2005), increasing demand of coal-based power plants (Garg et al., 2002; Prasad et al., 2006), ill-monitored industrial zones, emissions from biomass burning sources, and various household fuel consumption issues (Guttikunda et al., 2014).

CRB started in the year 1986 when mechanized harvesting for wheat (in the month of April–May) and rice (in the month of October–November) was started (Kaskaoutis et al., 2014; Sarkar et al., 2013; Singh & Kaskaoutis, 2014). CRB has recently gained a lot of traction due its substantial impact on seasonal air quality, particularly over the Indo-Gangetic Basin (IGB; Badarinath et al., 2006; Jain et al., 2014; Kaskaoutis et al., 2014; Liu et al., 2018; Ram et al., 2012; Singh & Kaskaoutis, 2014; Vijayakumar et al., 2016). In the year 2016, CRB and festival of light (Diwali) coincided that severely impacted weather of Delhi and surrounding areas and fog, haze, and smog were persistent for few weeks during last week of October and the first week of November (Chauhan & Singh, 2017). In the year 2017, the air quality over entire IGB in general and Delhi, in particular, had severe consequences from CRB in the states of Punjab and Haryana, in the northwestern part of IGB. The pollutants impacted visibility and caused toxic smog (Times, 2017) and prompted school closures for days to prevent exposure from the harmful pollutants. In addition, seasonal biomass or CRB also results in spiking of black carbon (BC) aerosols that has serious implications due to its ability to absorb incoming solar radiation and impact

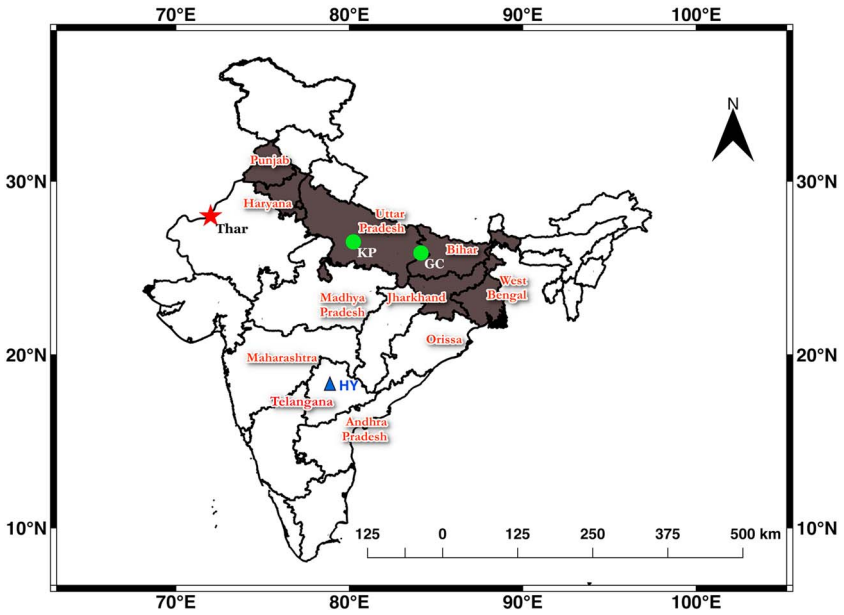

Figure 1. Map showing the study area and different states mentioned in the text. The green circles show locations of two AErosol RObotic NETwork stations (KP = Kanpur and GC = Gandhi College). The region shaded in dark gray represents the Indo-Gangetic Basin. The location of the Thar Desert (one of the largest dust source regions in India) has been shown with a red star. City of Hyderabad (HY) has been marked with a blue triangle.

climate (Babu & Moorthy, 2002; Babu et al., 2002; Bond et al., 2013; Menon, 2002; Ramanathan & Carmichael, 2008), human health (Gustafsson et al., 2009; Janssen, 2012), precipitation (Gautam et al., 2010; Meehl et al., 2008; Wang, 2007), and soil productivity (Rhodes et al., 2008). Many studies have focused on CRB and its impact on BC over IGB during the winter and postmonsoon period (October–November; Kaskaoutis et al., 2014; Kedia et al., 2014; Nair et al., 2007; Ramanathan, 2007). The increase in BC because of CRB has made the IGB region a global hot spot for atmospheric pollutants and a place for recurring winter haze and toxic fog.

While a lot of attention is given to the impact of CRB over the IGB region, less is known about the effect of CRB on the greater Indian peninsula. Kaskaoutis et al. (2014) and Kumar et al. (2015) discussed long-range transport of aerosols and BC over rest of India, focusing more on capturing the seasonal variations of these properties. Dumka et al. (2013) looked at the seasonal and diurnal variations of BC over the city of Hyderabad, located in the state of Telangana and found large seasonal fluctuations with wintertime peaks and summer lows. Similar studies have been carried out over other isolated locations in the central and southern part of India (Aruna et al., 2013; Babu & Moorthy, 2002; Kumar et al., 2011; Ramachandran & Rajesh, 2007; Safai et al., 2007, 2013, 2012). These studies, though mostly local in space and time, agree on the increase of BC during the postmonsoon and winter periods and the role of CRB in northwest India. In this paper, we have used data from multiple sources to study the changing aerosol pattern over larger parts of the Indian subcontinent and have documented increasing spatiotemporal extent and changing intensity of CRB in recent years.

2. Study Area

We have considered the whole of India (~8–40°N, 68–98°E; Figure 1) to study the impact of CRB (key states and regions that are referred to in this text have been highlighted in the figure).

3. Data

We have considered data from a number of satellite observations, ground stations, and global climate models to assess the impact of CRB over the Indian subcontinent, for the period 2003–2017. In some cases, depending on the availability of the data, the study periods are limited to years 2005–2016.

3.1. Satellite

We have used the Moderate Resolution Imaging Spectroradiometer (MODIS) active fire data, MOD14A2/MYD14A2 (Giglio & Justice, 2015) for detection of fire signals, during the postmonsoon season (October–November), over northwest India. This product is derived from the two MODIS instruments, which are on board the Terra and Aqua platforms of National Aeronautics and Space Administration (NASA) Earth Observation System (EOS). The collection 6 version of this data set, considered in this study, is an 8-day composite 1-km gridded product that represents the maximum value detected for each pixel within the entire 8-day compositing period. It was obtained from the Level 1 and Atmosphere Archive and Distribution System (http://ladsweb.nascom.nasa.gov). For each of the 8-day period, all pixels having the values of 8 and 9, representing, fire-nominal confidence and fire-high confidence, respectively, were summed to give the total count of observed fire for each year. The MODIS L3 tile h24v06, covering the northwestern region of India was considered for this purpose.

The multiwavelength single-scattering albedo (ω_0) data for the study area were obtained from the Ozone Monitoring Instrument sensor on board NASA's EOS Aura space platform. The 0.25° × 0.25° OMAEROe L3 product (Stein-Zweers & Veefkind, 2012; Version 3) provides a measurement of ω_0 at five different wavelengths, ranging from 342.5 nm to 483.5 nm. The L3 product selects the best aerosol values for each pixel, from all the input L2 good quality data, based on the shortest optical path length. These data were downloaded for the study period from the Goddard Earth Sciences Data and Information Services Center (https://disc.gsfc.nasa.gov). In addition to this, we have made use of aerosol optical depth and absorbing aerosol optical depth, measured at 500 nm, from the 1° × 1° OMAERUVd daily, L3 data set. This data set is based on an enhanced Total Ozone Mapping Spectrometer algorithm that uses the ultraviolet radiance data (Torres, 2008).

Methane is an inevitable by-product of CRB due to incomplete combustion. Changes in methane mixing ratios may indicate changing impacts of CRB. Vertical distribution of methane, across different pressure levels, has been obtained from the Atmospheric InfraRed Sounder (AIRS) on board the EOS Aqua platform. We have used the AIRS daily L3 product, AIRS3STD, which has global coverage at a spatial resolution of 1° × 1°. The AIRS instrument uses 2,378 spectral channels, between 3.74 and 15.4 μm, to provide vertical distribution of different trace gases and water vapor across the globe (AIRS Science Team, 2013).

We have used vertical profiles of aerosol extinction coefficients from the Cloud-Aerosol LIdar with Orthogonal Polarization instrument, on board the Cloud-Aerosol Lidar and Infrared Pathfinder Satellite Observations (CALIPSO) platform. CALIPSO is part of the NASA *A-Train* EOS system that was launched in April 2006. The vertical profiles of extinction coefficients have been obtained from level 2, version 4.0 aerosol profile products with a horizontal resolution of 5 km (Vaughan et al., 2009).

3.2. Model

The data for BC and dust column mass density were obtained from the Modern-Era Retrospective analysis for Research and Applications, Version 2 (MERRA-2) from the NASA's Global Modeling and Assimilation Office. MERRA-2 has an improved assimilation scheme compared to earlier MERRA system and is a long-term global reanalysis process that has a robust mechanism to assimilate satellite-derived observations of aerosols and their interactions with other physical processes (Gelaro et al., 2017). Besides, MERRA2 relies on a combination of satellite data and some high-resolution inventories to track time-dependent anthropogenic and biomass burning emissions. The data used in the present study are from the MERRA2 data set, M2TMNXAER (Global Modeling and Assimilation Office, 2015; obtained from the Goddard Earth Sciences data portal), which is a monthly mean spanning the entire globe, with a spatial resolution of 0.5° × 0.625°.

3.3. Ground Station

Specific ground-based aerosol measurements have been derived from the two AErosol RObotic NETwork (AERONET) stations located in the IGB, Kanpur, and Gandhi College (Figure 1). AERONET sites use CIMEL multiband Sun photometers to measure sun irradiance and sky radiances at eight spectral bands ranging from 340 to 1,020 nm (Holben et al., 2001). We have used the ω_0 data from the Version 3.0 Almucantar level 2.0 inversions and the Angstrom exponents (α) from the Version 2.0 direct Sun measurements.

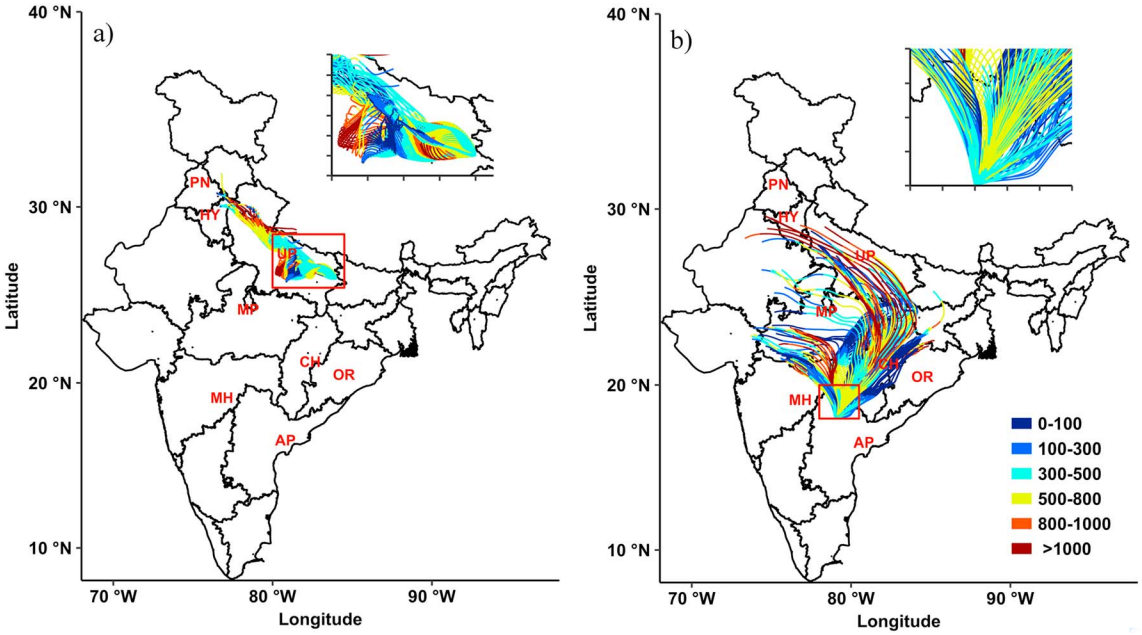

Figure 2. HYbrid Single Particle Lagrangian Integrated Trajectory back trajectory calculation for two locations, over the (a) eastern parts of Indo-Gangetic Basin and (b) central south India (b). The matrix locations are shown with red rectangles in each of the figures, and the inset figures show greater detail of the trajectories over the matrix locations. The two-letter state abbreviations, given in red, stands for PN = Punjab; HY = Haryana; UP = Uttar Pradesh; MP = Madhya Pradesh; MH = Maharashtra; AP = Andhra Pradesh; CH = Chattisgarh; OR = Odisha. These simulations were initiated for 5 November 2016 and were allowed to run for 240 hr.

4. Trend Estimates

The trends for ω_0, dust, and BC have been computed, using a Mann-Kendall test for detection of monotonic trends in the time series (Hirsch & Slack, 1984; Mann, 1945). The slope for these trends has been estimated through a nonparametric Theil-Sen statistic (Sen, 1968) that is equivalent to the least squares regression but like the Mann-Kendall test that is free from the assumption of normal distribution. Both of these tests have been shown to be more robust to the presence of outliers in the time series. We have followed a similar methodology as discussed by Sarkar (2017) and have used the NCL package (https://www.ncl.ucar.edu) for the estimation of the actual trends. All trends, presented in this work, are interannual trends that have been computed for the postmonsoon CRB period lasting from October to November of each year.

5. Prevailing Wind Pattern

The dominant wind pattern during the postmonsoon and winter period in India is northerly to northwesterly. This wind mostly originates from the north, northwestern region of India where a high-pressure system prevails during this time, because of low temperatures and divergence induced by the subtropical jet stream (see Figure S1 in the supporting information). Back trajectories, computed using the HYbrid Single Particle Lagrangian Integrated Trajectory model (Draxler & Rolph, 2003), over two locations, in IGB, and in Central India, confirm this outgoing northerly and northwesterly wind pattern (Figure 2). These back trajectories were modeled using wind profile data from the $1° \times 1°$ Global Data Assimilation System data, for 5 November 2016. The models were run for 240 hrs with initial height fixed at 500 m. Figure 2 shows that the back trajectories from both the locations point to northwestern India, toward the states of Haryana and Punjab. The trajectories that are color coded by height (in meters above ground level) show that most of the pollutants are transported from north-northwest India at heights below 500 m or less, which is mostly well within the planetary boundary layer height that is prevalent during the postmonsoon period (Patil et al., 2013). This also agrees with similar observations that have been made over other biomass burning areas where most of the aerosol load was found to be restricted within the mixing layer with rare evidence of injection to the free troposphere (Bikkina et al., 2016; Labonne et al., 2007; Ram et al., 2010). We do see some evidence of long-range transport at heights above the boundary layer, especially for the location in central India, suggesting that BC aerosol-laden winds can travel longer distances at higher altitudes and impact far off places.

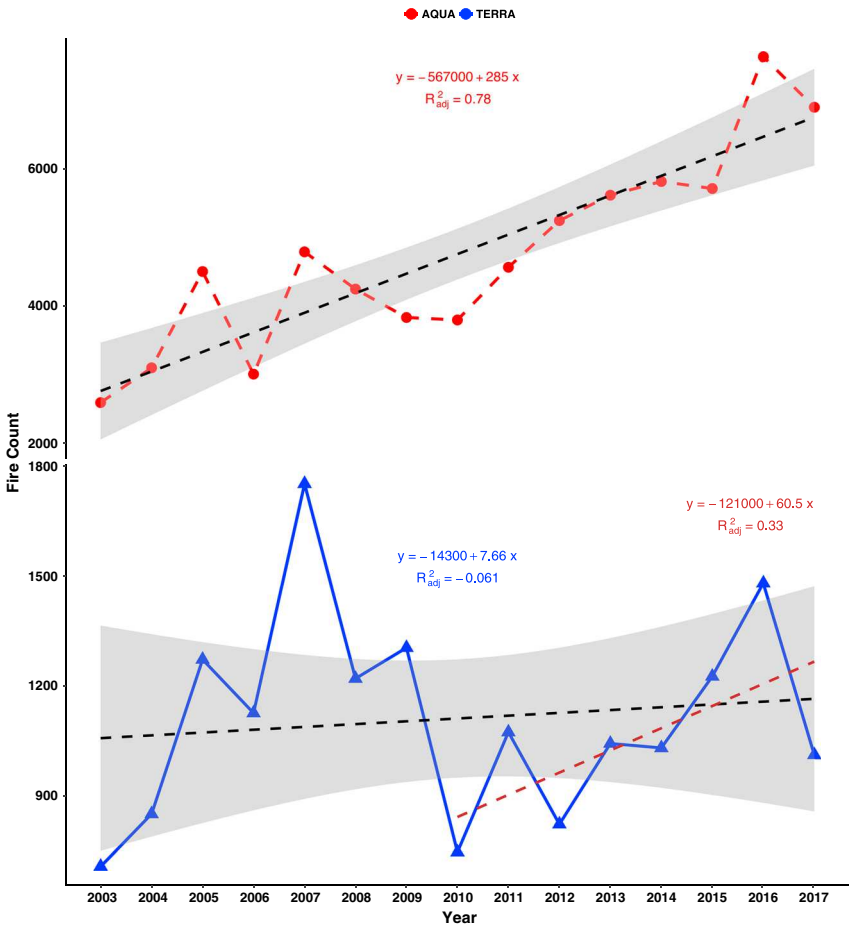

Figure 3. Fire count, accumulated between days 273 and 336, for years 2003 to 2017 from TERRA and AQUA. These data were compiled from MODIS tile h24v06 that cover the northwestern states where CRB during the postmonsoon period is prevalent. The linear regression trend fit for both TERRA and AQUA, for the entire study period has been shown in black dashed lines. For TERRA another trend fit, since 2010, has been shown in brown dashed line. The linear regression equations and R^2_{adj} values for each fit are shown in the figure with the 95% confidence interval shown as a gray shaded interval. AQUA detects higher fire counts and a statistically significant increasing trend since 2003, whereas TERRA does not show much trend overall but does show a weak increasing trend after 2010.

6. Observed Trends

6.1. Fire Counts

The yearly total fire counts, as measured from the MODIS active fire data sets (M*D14A2), over the northwestern part of India, show a distinct trend, primarily, since the year 2010. The yearly fire counts, cumulated over the postmonsoon (October–November) season for every year, have been fitted with a linear trend and the slope and adjusted *r*-squared (R^2_{adj}) values are shown in Figure 3. An increasing trend is seen for the entire study period, since the year 2003, for Aqua MODIS (hereafter referred to as AQUA) with the R^2_{adj} value of 0.78 (*p* value: 7.15e−06). For Terra MODIS (hereafter referred to as TERRA), no such trend is observed, although we observe some increase in fire counts for TERRA, since 2010, though not statistically significant (R^2_{adj} value of 0.33, *p* value: 0.08). Both AQUA and TERRA show peaking of fire counts in the year 2016. The AQUA derived yearly magnitudes are also seen to be much higher than TERRA. This observation of higher fire counts measured by AQUA is consistent with findings of Kaskaoutis et al. (2014), who found that count of fire pixels from AQUA was about 10 times higher than those of TERRA over the state of Punjab. TERRA is a morning satellite with local overpass time of 10:30 a.m., while AQUA has an afternoon overpass time of 1:30 p.m. We conjecture that because of this difference in observation time, AQUA can detect more fires as CRB picks

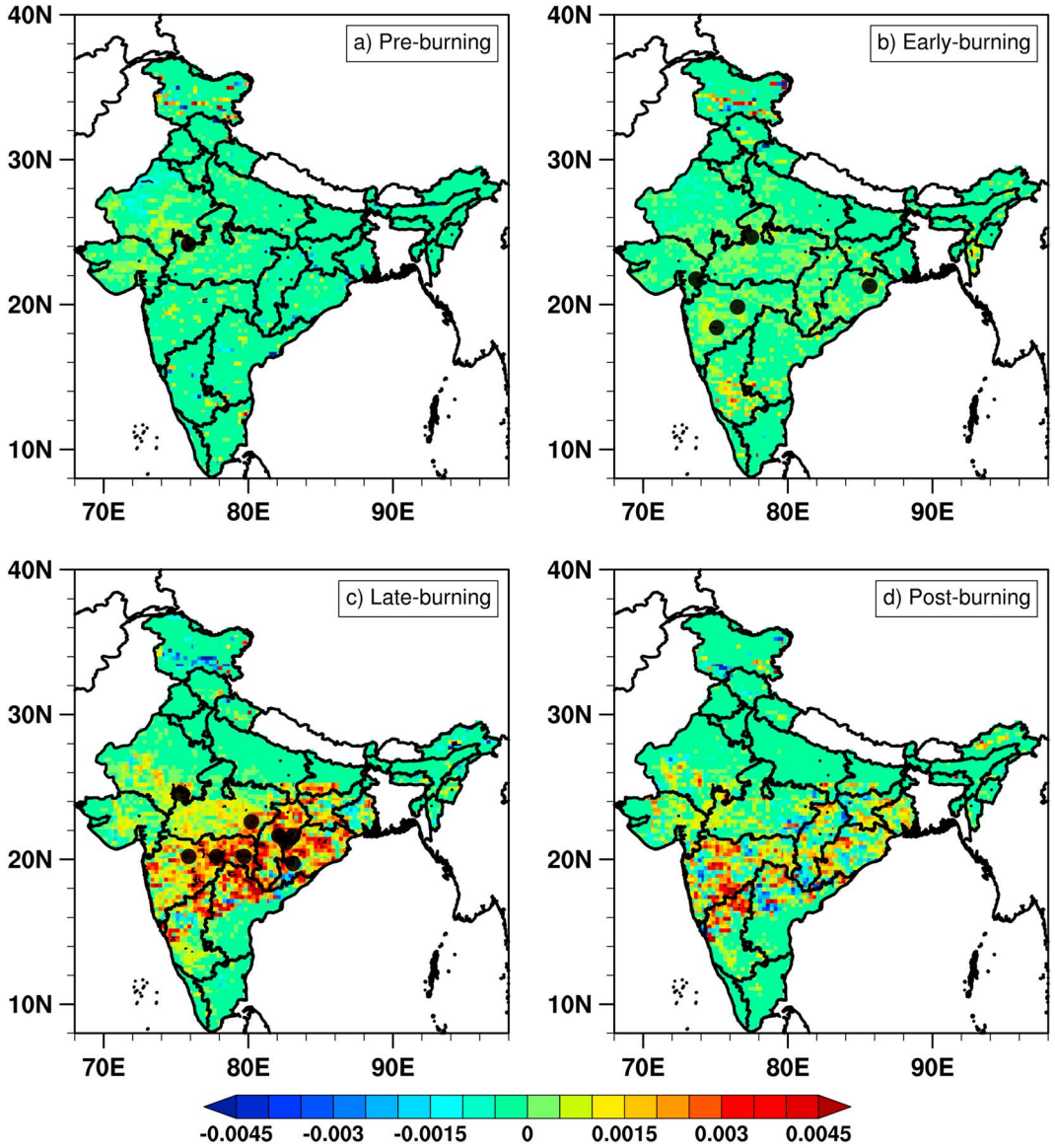

Figure 4. Temporal trend of ω_0 calculated at four subperiods, as defined by Kaskaoutis et al. (2014). Black circles are placed over areas where the trend is significant at 95%. Late burning period (1–17 November) shows increasing trend of ω_0 (λ_{463}). This is derived from the OMAEROe data set.

up with the progression of the day. It is a common practice of farmers to begin burning in the morning and end by the evening. Nonetheless, irrespective of the differences in the magnitude of fire counts both TERRA and AQUA observations show a matching increasing trend in the period after 2010–2011.

6.2. Trend of ω_0

Kaskaoutis et al. (2014), divided the primary postmonsoon CRB season into four subperiods, based on number of fire counts, intensity of burning and aerosol loading into (a) preburning (1–15 October 2012), (ii) early burning (15–30 October 2012), (iii) late burning (1–17 November 2012), and (iv) postburning (18–30 November 2012). We considered their classification and looked at the trend of ω_0 (λ_{463}) in each of these four subperiods (Figure 4), based on the OMAEROe daily L3 data set. Average for each of the four periods was computed from the daily data set, and a Mann-Kendall slope was fitted at each point. Black circles in Figure 4 indicate all areas where the trend is significant at 90%, based on the Theil-Sen trend statistic. Out of all the four subperiods considered, the late burning period shows clear evidence of an increasing trend

in ω_0 at the blue-ultraviolet region of the spectrum. This increase is seen over the central southern regions of India, covering the states of Madhya Pradesh, Maharashtra, Chhattisgarh, Odisha, and northern Andhra Pradesh (now referred to as Telangana; Figure 1).

6.3. Trend of BC and Dust

There are mainly two dominant sources of long-range pollutants in India, which are BC and dust (Dey et al., 2004; Singh et al., 2004). BC aerosols mostly comprise fine particles (0.1–1 μm) that are residuals from incomplete burning as in fossil fuel, biogenic-fuels and CRB (Collins, 2002). Given their small size, BC aerosols are more prone to long-range transport and have a longer life in the atmosphere. Dust comprises larger particles of size 2 μm or more. Dust is more strongly absorbing at lower wavelengths, which cannot explain the increase in ω_0 (λ_{463}) that is seen in Figure 4. But at the same time, both dust and BC aerosols can claim their provenance from northwestern India. We estimated the trend of dust and BC column mass density from the MERRA2 data, for November (Figure 5). The meridional variation of BC and dust column density anomalies along 77E longitude are shown in Figures 5c and 5d, respectively. Stippled areas in Figures 5a and 5b show significant trend (95% confidence level).

From the BC and Dust trends we found:

- An increasing trend in dust aerosols is largely confined to their source regions of western and northwestern India (Figure 5b). Most of the dust particles owe their source to the Thar Desert and long-range transport from the Sahara region, which makes a pathway through the northwestern states of India.
- On the contrary, the increase in BC is more evident along the eastern IGB and central India, conforming to the northwesterly wind direction in the postmonsoon period (Figures 5a and S1).
- From Figure 5d, we can see that dust event are more pronounced around the premonsoon period (March to early June), and the influx of dust to lower latitudes is less frequent and is seen only a few times during 2005–2016, mainly in 2008 and 2012. This conforms to findings of Gautam et al. (2009). Pandey et al. (2017) have also reported this decline of premonsoon dust events.
- An influx of BC at lower latitudes is far more common, and we observe more BC spikes on and after the year 2010.

Source apportionment of BC, especially in South Asia, can be problematic (Gustafsson et al., 2009) because of multiple emission sources for fine mode particles. Thus, the increase in BC along the eastern part of the IGB and central southern regions may be potentially attributed to a number of different sources with CRB being one of them. However, the month-wise trend of BC, as shown in Figure 5a, but computed for each month of the year (see Figure S2 in the supporting information) shows the pronounced increase in the month of November in the eastern and central south regions. Furthermore, the area of increase conforms to the contours of prevailing wind direction at this time of the year (Figures 2 and S1 in the supporting information). In general, the most widespread increase in BC over the eastern and central south regions is seen in the postmonsoon and winter periods, thus confirming the greater role of transport of BC from northwesterly source regions in during this time. Our conclusions agree with Dumka et al. (2013), who attributed the wintertime peak in BC at Hyderabad to crop residue and biomass burning in the northwestern regions. They opined that such seasonality in BC concentrations might not be caused by any local anthropogenic sources, as anthropogenic emissions remain continuous throughout the year. We rule out any role of local large-scale biomass burning in the central south regions for postmonsoon BC enhancements, as CRB in the central south regions is largely prevalent between February and May, peaking in the month of March. Comparing month-wise fire counts from the Global Fire Emissions Database (GFED 4s; van der Werf et al., 2017) for the IGB and central south regions corroborates this (ref: Figure S3 in the supporting information).

7. Changes in Methane Emissions

Methane emission can result from incomplete combustion of biofuels or crops and is particularly relevant for paddy leftover burning in the northwestern India, where anaerobic conditions, prevailing in submerged paddy fields, can create a pool of methane (Bhatia et al., 2013). To assess the relative magnitude of methane emissions, from CRB, over northern and central south regions of India, we looked at methane emissions from different sources based on Emissions Database for Global Atmospheric Research (Crippa et al., 2016; EDGAR 431: European Commission, Joint Research Centre/Netherlands Environmental Assessment Agency (PBL),

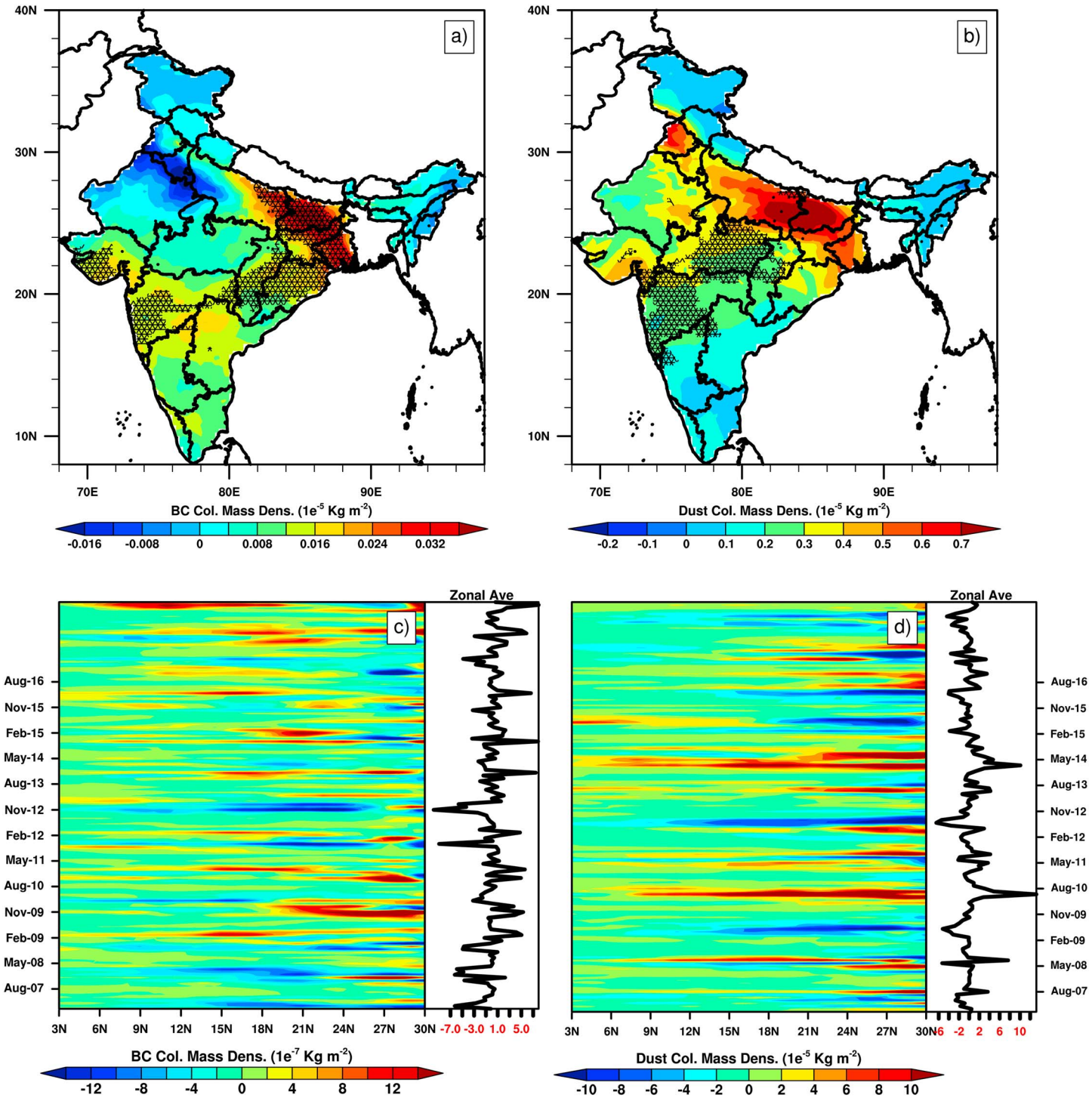

Figure 5. Temporal trend for (a) black carbon and (b) dust column mass density, for November, as obtained from the monthly Modern-Era Retrospective analysis for Research and Applications, Version 2 data set, M2TMNXAER. Stippled areas represent places where the trend is significant at 95%. Time-latitude profiles showing the yearly variation of respective column mass density anomalies, along 77°E longitude, are shown in (c) for black carbon and in (d) for dust. The meridional averages are shown on as line plots with each of these figures.

2016) data. We considered emissions from enteric fermentation, agricultural soils, agricultural waste burning, fossil fuel combustions, manures, road transportation, and solid wastes. The emission from each source was normalized, and the annual increase from each source was divided by the gross increase from all emission

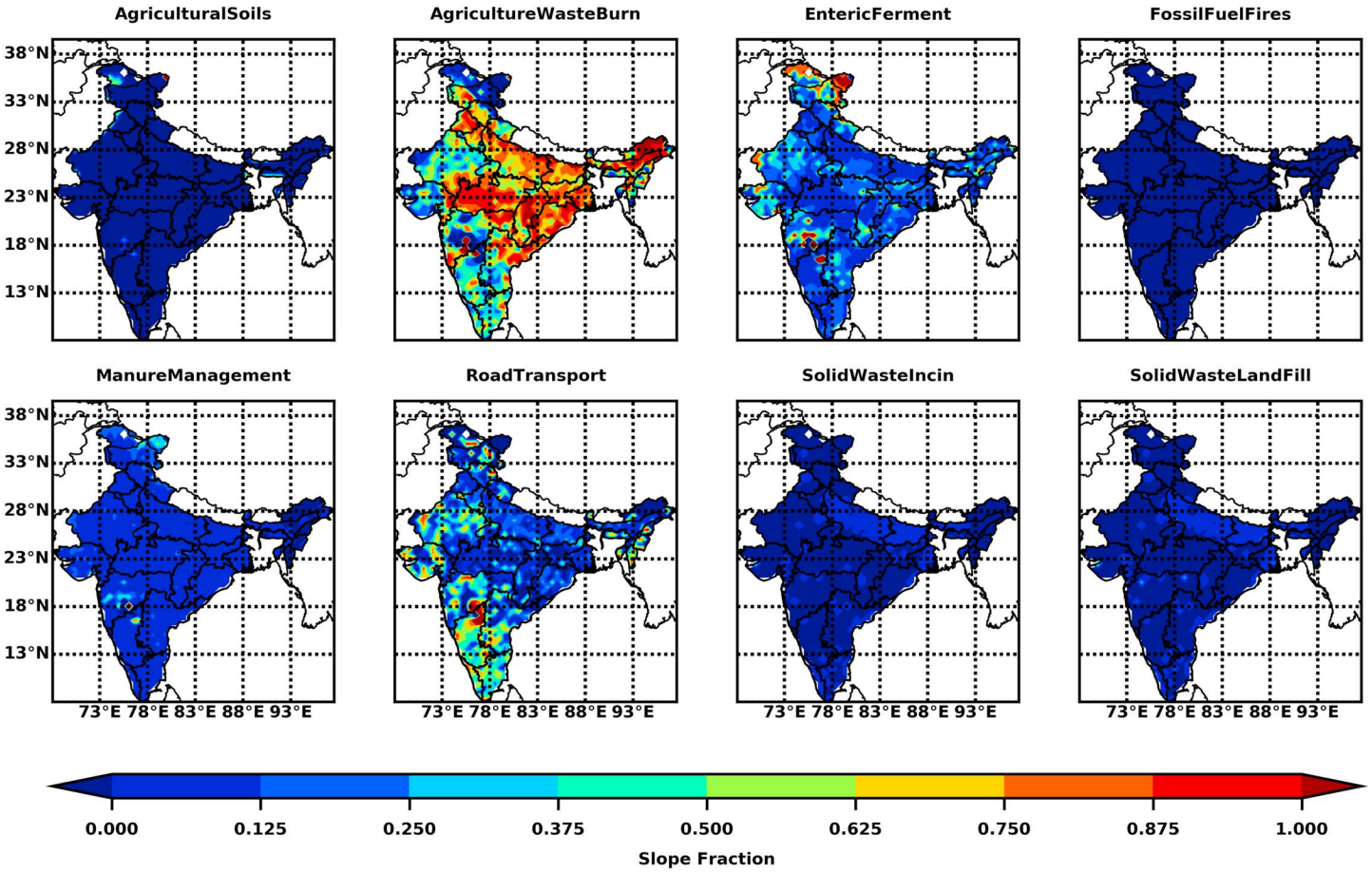

Figure 6. The relative increase of methane emissions from different sources, derived from the Emission Database for Global Atmospheric Research 431. This is shown as slope fraction for each emission component, defined as the trend slope of a particular emission component divided by the sum of trend slopes from all emission components. All emission components were normalized to minimize bias.

sources. Figure 6 shows the fractional increase of methane emission from each source; the maximum increase in methane emission is found from agricultural waste burning over the IGB and central southern regions.

We looked at the changes in methane volume mixing ratios, derived from the ascending (daytime) mode of AIRS sensor. We considered vertical variations of methane between 12°N and 22°N latitudes and along 77°E longitude. The daily methane observations were converted to monthly averages, and the departures from monthly means were estimated as monthly anomalies. We found an increase in methane mixing ratios (Figure 7a), on and after the postmonsoon period of the year 2010. A meridional profile of monthly anomalies of Ozone Monitoring Instrument derived ω_0 (λ_{463}) computed between 16°N and 24°N for November (Figure 7b) shows higher values of ω_0 (λ_{463}) in lower latitudes, being more prevalent on and after the year 2009. The timing of this increase is similar to the increase in methane volume mixing ratio (Figure 7a) and agrees with the trend in AQUA derived fire counts (Figure 3).

8. Closer Studies of Aerosol Type and Characteristics

8.1. AErosol RObotic NETwork

Delineation of aerosol source and type is possible based on consideration of wavelength dependent factors like α_λ and ω_0. The AERONET data from Kanpur and Gandhi College, both located in the eastern parts of IGB, have been used to look at the aerosol characteristics and how it has evolved at these two AERONET locations. Figure 8 shows the variation of α_λ, calculated from direct Sun algorithm (Holben et al., 2001), at 500–870 nm

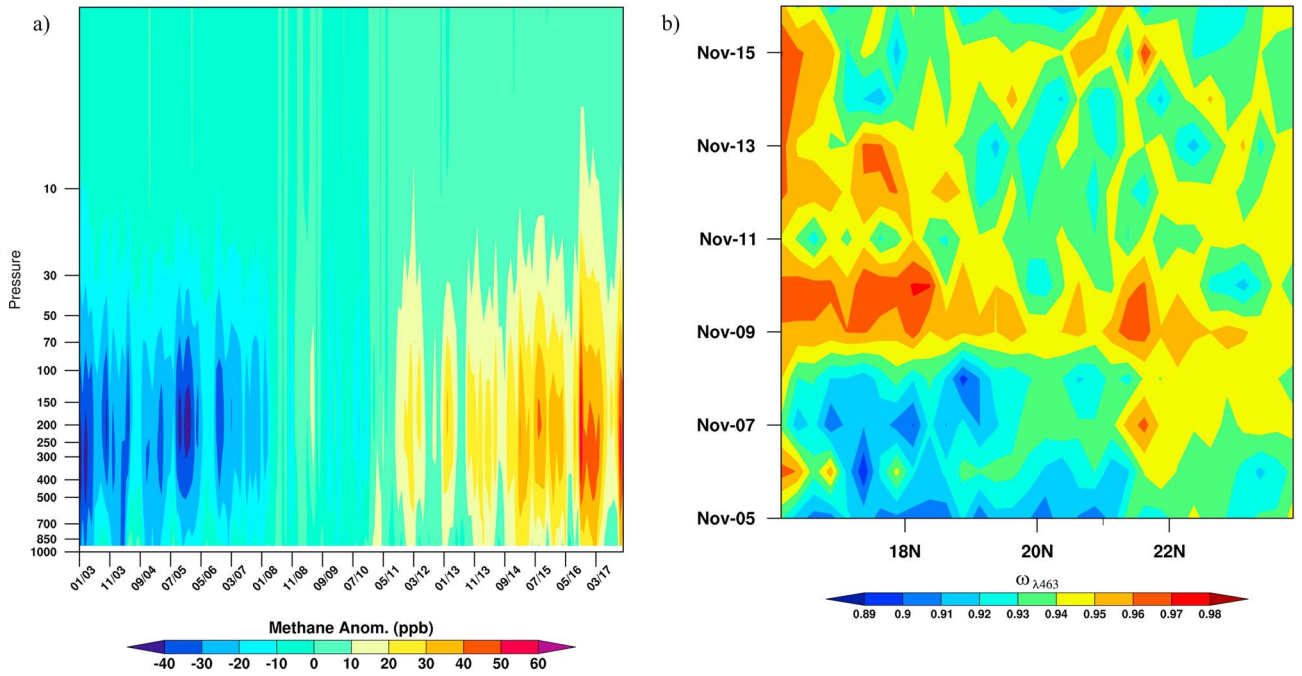

Figure 7. (a) Pressure (hPa)—time profile of methane volume mixing ratio anomalies, over 12–22°N latitude and along 77°E longitude. Two prominent phases of increase in methane volume mixing ratio are detected, during 2010 to 2013, and further increase since 2013 to present. (b) Time-latitude profile showing the variation of ω_0 (λ_{463}) for November, as derived from the OMAEROe data set between 16°N and 24°N and along 77°E longitude. We see a marked increase in ω_0 south of 20 N, from 2010 onward.

($\alpha_{500-870}$) and 340–440 nm ($\alpha_{340-440}$), at (a) Gandhi College and (b) Kanpur. A trend line has been fitted to each curve based on loess regression, which is a robust smoothing algorithm based on local polynomial regression. The $\alpha_{500-870}$ for Gandhi College shows an increasing trend since the year 2010 whereas $\alpha_{340-440}$ decreases slightly, at the same time. For Kanpur, the same trend is observed, but it is not as prominent as

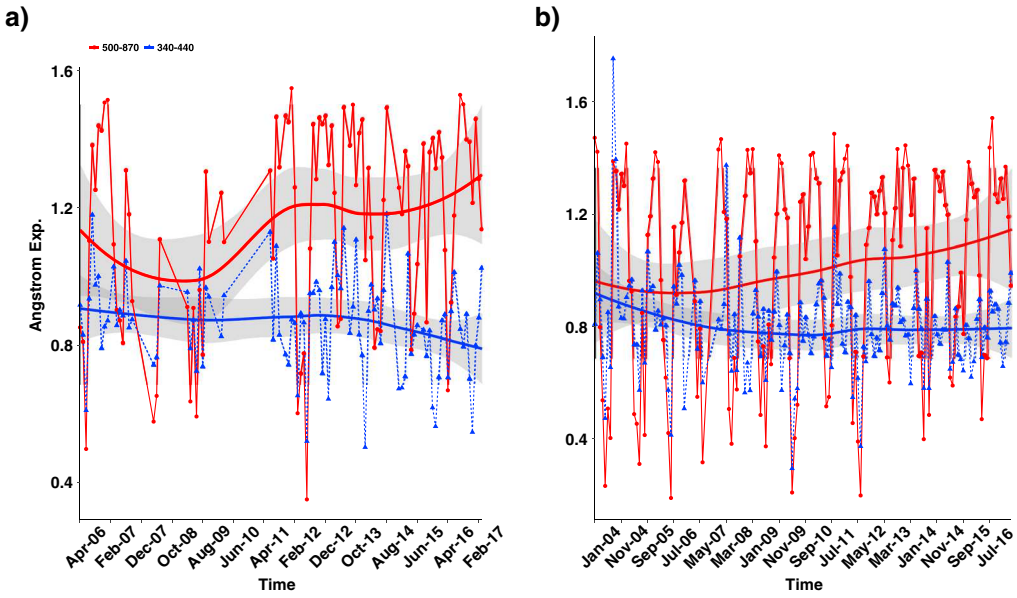

Figure 8. Plot of $\alpha_{500-870}$ and $\alpha_{340-440}$ for two AErosol RObotic NETwork sites of (a) Gandhi College and (b) Kanpur. A sharp increase in seen in $\alpha_{500-870}$ for Gandhi College, during 2009 to 2011 and again from 2014 onward. In Kanpur, the trend is little subdued for reasons that have been described in the text.

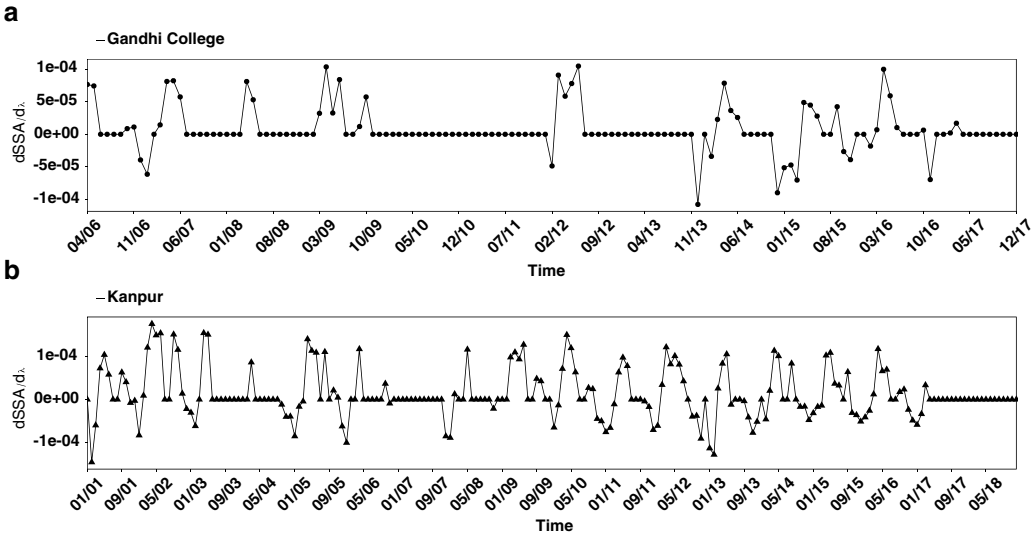

Figure 9. Variation of $\delta\omega_0/\delta\lambda$, estimated at wavelengths of 440, 675, 870, and 1,020 nm for two AErosol RObotic NETwork stations of (a) Gandhi College and (b) Kanpur.

Gandhi College. The 830- to 880-nm wavelength range is considered as the optimal wavelength range for BC aerosol estimation as BC aerosols are most sensitive in this range (Sreekanth et al., 2007). The increase of $\alpha_{500-870}$ values, away from 1, toward 1.5 and higher indicates a greater preponderance of finer mode particles, including sulfates, nitrates, ammonium, organic carbon, and BC, in recent years. A similar increase in finer particles is observed through an analysis of the AERONET-based fine mode fractions data (not shown) that are based on a spectral deconvolution algorithm (O'neill, 2003).

BC aerosols are more absorptive in visible and near-infrared ranges and exhibit more scattering in blue and ultraviolet regions of the spectrum. This dependence of ω_0 with wavelength ($\delta\omega_0/\delta\lambda$) has been estimated at four wavelengths, ranging from 440 to 1,020 nm, based on AERONET measurements (variations are shown for Gandhi College in Figure 9a and for Kanpur in Figure 9b). The values of $\delta\omega_0/\delta\lambda$ that are <0 are indicative of the presence of BC. From the variation of $\delta\omega_0/\delta\lambda$, we observe

1. In Gandhi College, a more regular pattern of negative slope values, around the postmonsoon and winter period of every year. Whereas the positive peaks, indicative of dust spikes are seen around the premonsoon months from March to May.
2. In Kanpur, the pattern is more irregular similar to variations of α in Figure 8.
3. An increasing frequency of negative slope values, after winter of 2010 compared to earlier periods, which is evident from the Gandhi College observations.

Kanpur is an industrial city, where the source of aerosol, especially BC aerosol is complicated by various other emission sources like automobiles, power plants, brick kilns, multiple industries, and indoor fuel consumption (Singh et al., 2004). So no clear pattern emerges in Kanpur of variation of BC, solely from CRB. The variation of ω_0 in Kanpur also shows an increasing effect of dust and brown carbons that are known to be more absorptive in the lower wavelength ranges compared to BC.

8.2. Other Satellite- and Ground-Based Observations

Figure 10a shows area averaged aerosol absorption coefficients, derived over central India, over a bounding box, centered on 22°N and 77°E. These are derived from CALIPSO vertical profiles of extinction coefficients at 532 nm that were scaled, based on factors estimated from colocated observations of absorbing aerosol optical depth and aerosol optical depth, obtained from OMAERUVd at 500-nm wavelength. The data are shown for two days, 24 October (early burning) and 9 November (late burning) in 2016. Most of the changes related to CRB are seen to be restricted within the lower 2 km of the atmosphere. We observe a substantial jump in the absorption coefficient of 50% or more in these central Indian regions from early burning to late burning period.

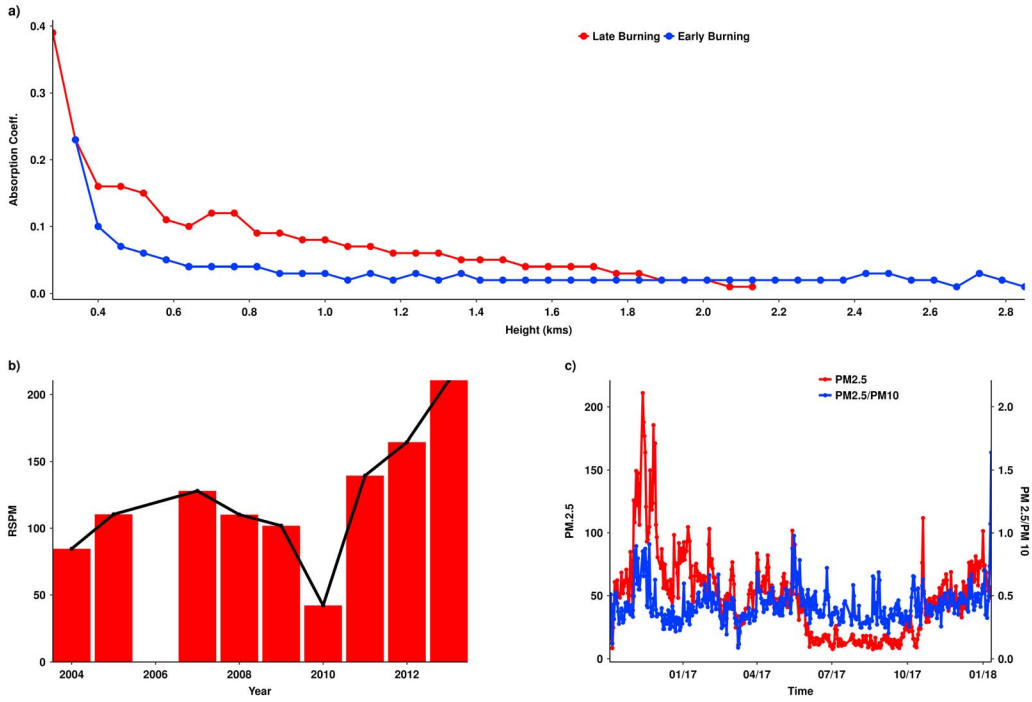

Figure 10. (a) Variation of aerosol absorption coefficient with height for a box centered on 22°N and 77°E. The absorption coefficients have been derived from Cloud-Aerosol Lidar and Infrared Pathfinder Satellite Observations extinction coefficients at 532 nm and scaling them by factors obtained through colocated absorbing aerosol optical depth and aerosol optical depth observations from OMAERUVd. (b) Monthly average value for Respirable Suspended Particulate Matter, for November, for a site (C.I.T.D. Balanagar) in the city of Hyderabad (~17.4 N, 78.5°E) within Telangana state. (c) The diurnal variation of PM2.5 (red) and PM2.5/PM10 ratio (blue), for a site in the city of Aurangabad (19.8 N, 75.3°E; station name: More Chowk-Waluj) in the state of Maharashtra. We observe peaking of PM2.5 and PM2.5/PM10 ratio between November to December of 2016 and 2017, increase for 2016 was highest.

Implications of BC enhancement in the postmonsoon ambient air quality, over the eastern and Central India, are far reaching. Unfortunately, there are not enough ground stations in India that provide long-term data of PM2.5 and PM2.5/PM10 ratio over the years. Changes in such ratio are reflective of the changing fraction of fine mode particles and could imply changing BC concentration in ambient air. We considered one station located in the city of Hyderabad (Figure 1), maintained by the Central Pollution Control Board of Government of India. Figure 10b shows variations of Respirable Suspended Particulate Matter (RSPM) for November. All available valid daily values for the month were averaged to obtain the monthly total for a given year. RSPM indicates particles that are small enough ($<$2.5 μm) to pass through nasal hairs and reach human lungs. Though the data shown in Figure 10b are not complete and are available only until the year 2013, it shows a steady increase in RSPM from the year 2011 onward. It may be noted that some of these stations are poorly maintained, and instruments may not be routinely calibrated; however, the steady increase in RSPM after 2010 is likely associated with changing BC/finer particles concentrations in the atmosphere of central India during winter time. Figure 10c shows the diurnal variation of PM2.5 and PM2.5/PM10 fractions, during the years 2016 and 2017, for another site located in the state of Maharashtra, in central India. It shows an increase in values of finer particles, starting from end October to December of each year. The increase in 2016 was the highest, corresponding to the highest number of fires that were observed for the year 2016 (Figure 3).

9. Summary and Conclusion

Increased episodes of CRB in the north and the northwestern regions of India have been confirmed by the analysis of a number of satellite- and ground-based observations. Mechanized harvesting leaves more residues in the field in the form of stalks, stubbles, and straws that are burnt by the farmers to clear the field for next crop. It is known that residue generation and burning are proportional to mechanized rice cultivation systems (Kumar et al., 2014; Manjunatha et al., 2015; Sharma & Prasad, 2008). Hence, an increase in CRB could

be the result of an increased shift toward mechanized harvesting, which has gradually spread, over the years, to other states including foothills of Himalaya. This air mass, contaminated from the CRB, is reaching over the eastern and central parts of India. Even the rice producing eastern states of India have increasingly resorted to CRB in recent years. It is evident from Figures 3, 5a, 8, and 9 that the post-2010 growth spurt in CRB has come in two episodes. The first episode roughly lasts from the year 2010 to the year 2013, and then we see another uptick from 2014 onward, which reflects increasing shift toward mechanized harvesting in recent times. The recent regulations, put forth to curb these widespread practices of CRB (DTE, 2017; Urmila, 2017), may explain the slight dip in the count of fires that we observed for the year 2017 (Figure 3).

Our results clearly show an increased preponderance of BC aerosols and finer particles, during the postmonsoon and wintertime, over the eastern IGB and central India. Comparing the seasonality of other emission sources and fire events in central south regions based on emission inventory sources like EDGAR and Global Fire Emissions Database, we show that increase in methane and BC during November over central south regions has to come from source areas located in north-northwestern India.

Most impacted is the period during the first and second week of November when the northwesterly winds are seen to transport burning residues and alter the ambient air quality over these parts of India. This deterioration of air quality is of great concern especially over the Eastern IGB that is already riddled with increasing pollution from various other sources like coal mining, fossil fuel combustion, industrial outputs, and increased vehicular traffic, all of which are contributors to BC and brown carbon.

Acknowledgments
The authors are grateful to MODIS, AIRS science team for providing satellite data, and to NASA AERONET team for providing Kanpur and Gandhi College AERONET data for the present study. Kanpur AERONET station was established by one of the authors (R. P. S.) through a joint Memorandum of Understanding between Indian Institute of Technology (IIT) Kanpur and NASA, Maryland. Thanks to Brent Holben PI of the AERONET program. We are also thankful to NOAA ARL for making the HYSPLIT model available for use. The first author (S. S,) is thankful to Sadashiva Devadiga and Keith Duffy from SSAI for their continued support and patronage. The authors are grateful to three anonymous reviewers and Editor for their constructive comments/suggestions that have helped us to improve earlier version of the paper. All data used in this study are publicly available and have been duly cited in this text. All supporting figures (Figures S1–S3) can be found in the supporting information section. The analysis presented in this text has carried out through NCL (https://www.ncl.ucar.edu), Python, and R. The R code to plot the wind back trajectories from HYSPLIT end points file can also be found as part of the supporting information. Thee first author (S. S.) built and conceptualized upon the notion that was first put forward by second author (R. P. S.). S. S. planned and executed the actual research. R. P. S. and S. S. wrote the manuscript. and R. P. S. also helped in senior review. The third author (A. C.) helped with analysis and collection of station data.

References

AIRS Science Team/Joao Texeira (2013). AIRS/Aqua L3 daily standard physical retrieval (AIRS-only) 1 degree × 1 degree V006, Greenbelt, MD, USA, Goddard Earth Sciences Data and Information Services Center (GES DISC), Accessed [2018]. https://doi.org/10.5067/Aqua/AIRS/DATA303

Aruna, K., Kumar, T. L., Rao, D. N., Murthy, B. K., Babu, S. S., & Moorthy, K. K. (2013). Black carbon aerosols in a tropical semi-urban coastal environment: Effects of boundary layer dynamics and long range transport. *Journal of Atmospheric and Solar-Terrestrial Physics*, *104*, 116–125. https://doi.org/10.1016/j.jastp. 2013.08.020

Babu, S. S., & Moorthy, K. K. (2002). Aerosol black carbon over a tropical coastal station in India. *Geophysical Research Letters*, *29*(23), 2098. https://doi.org/10.1029/2002GL015662

Babu, S. S., Satheesh, S. K., & Moorthy, K. K. (2002). Aerosol radiative forcing due to enhanced black carbon at an urban site in India. *Geophysical Research Letters*, *29*(18), 1880. https://doi.org/10.1029/2002GL015826

Badarinath, K., Kharol, S. K., & Sharma, A. R. (2009). Long-range transport of aerosols from agriculture CRB in Indo-Gangetic Plains—A study using LIDAR, ground measurements and satellite data. *Journal of Atmospheric and Solar-Terrestrial Physics*, *71*(1), 112–120. https://doi.org/10.1016/j.jastp. 2008.09.035

Badarinath, K. V. S., Kiran Chand, T. R., & Krishna Prasad, V. (2006). Agriculture CRB in the Indo-Gangetic Plains—A study using IRS-P6 AWiFS satellite data. *Current Science*, 1085–1089.

Badhwar, N., Trivedi, R. C., & Sengupta, B. (2006). Air quality status and trends in India, paper presented at better air quality workshop. *Clean Air Initiative for Asian Cities, Yogyakarta,* Indonesia 13–15.

Bhatia, A., Jain, N., & Pathak, H. (2013). Methane and nitrous oxide emissions from Indian rice paddies, agricultural soils and CRB. *Greenhouse Gases: Science and Technology*, *3*(3), 196–211. https://doi.org/10.1002/ghg.1339

Bikkina, S., Andersson, A., Sarin, M. M., Sheesley, R. J., Kirillova, E., Rengarajan, R., et al. (2016). Dual carbon isotope characterization of total organic carbon in wintertime carbonaceous aerosols from northern India. *Journal of Geophysical Research: Atmospheres*, *121*, 4797–4809. https://doi.org/10.1002/2016jd024880

Bond, T. C., Doherty, S. J., Fahey, D. W., Forster, P. M., Berntsen, T., Deangelo, B. J., et al. (2013). Bounding the role of black carbon in the climate system: A scientific assessment. *Journal of Geophysical Research: Atmospheres*, *118*, 5380–5552. https://doi.org/10.1002/jgrd.50171

Chauhan, A., & Singh, R. P. (2017). Poor air quality and dense haze/smog during 2016 in the indo-gangetic plains associated with the CRB and Diwali festival. In *2017 IEEE International Geoscience and Remote Sensing Symposium (IGARSS)*. https://doi.org/10.1109/igarss.2017.8128389

Collins, W. D. (2002). Simulation of aerosol distributions and radiative forcing for INDOEX: Regional climate impacts. *Journal of Geophysical Research*, *107*(D19), 8028. https://doi.org/10.1029/2000JD000032

Crippa, M., Janssens-Maenhout, G., Dentener, F., Guizzardi, D., Sindelarova, K., Muntean, M., & Granier, C. (2016). Forty years of improvements in European air quality: Regional policy-industry interactions with global impacts. *Atmospheric Chemistry and Physics*, *16*(6), 3825–3841. https://doi.org/10.5194/acp-16-3825-2016

Dey, S., Tripathi, S. N., Singh, R. P., & Holben, B. N. (2004). Influence of dust storms on the aerosol optical properties over the Indo-Gangetic Basin. *Journal of Geophysical Research*, *109*, D20211. https://doi.org/10.1029/2004JD004924

Draxler, R. R., & Rolph, G. D. (2003). HYSPLIT (HYbrid Single-Particle Lagrangian Integrated Trajectory). NOAA Air Resources Laboratory, Silver Spring, MD. Model access via NOAA ARL READY Website.

DTE (2017). India's burning issue of crop burning takes a new turn. Retrieved from http://www.downtoearth.org.in/coverage/river-of-fire-57924

Dumka, U., Manchanda, R., Sinha, P., Sreenivasan, S., Moorthy, K., & Babu, S. S. (2013). Temporal variability and radiative impact of black carbon aerosol over tropical urban station Hyderabad. *Journal of Atmospheric and Solar-Terrestrial Physics*, *105-106*, 81–90. https://doi.org/10.1016/j.jastp.2013.08.003

EDGAR 431: European Commission, Joint Research Centre/Netherlands Environmental Assessment Agency (PBL) (2016). Emission Database for Global Atmospheric Research (EDGAR), release version 4.3.1 http://edgar.jrc.ec.europa.eu/overview.php?v=431

Garg, A., Kapshe, M., Shukla, P., & Ghosh, D. (2002). Large point source (LPS) emissions from India: Regional and sectoral analysis. *Atmospheric Environment*, *36*(2), 213–224. https://doi.org/10.1016/s1352-2310(01)00439-3

Gautam, R., Hsu, N. C., & Lau, K. (2010). Premonsoon aerosol characterization and radiative effects over the Indo-Gangetic Plains: Implications for regional climate warming. *Journal of Geophysical Research*, *115*, D17208. https://doi.org/10.1029/2010JD013819

Gautam, R., Hsu, N. C., Lau, K., Tsay, S., & Kafatos, M. (2009). Enhanced pre-monsoon warming over the Himalayan-Gangetic region from 1979 to 2007. *Geophysical Research Letters*, *36*, L07704. https://doi.org/10.1029/2009GL037641

Gelaro, R., Mccarty, W., Suárez, M. J., Todling, R., Molod, A., Takacs, L., et al. (2017). The Modern-Era Retrospective Analysis for Research and Applications, Version 2 (MERRA-2). *Journal of Climate*, *30*(14), 5419–5454. https://doi.org/10.1175/jcli-d-16-0758.1

Ghude, S. D., Chate, D. M., Jena, C., Beig, G., Kumar, R., Barth, M. C., & Pithani, P. (2016). Premature mortality in India due to PM2.5 and ozone exposure. *Geophysical Research Letters*, *43*, 4650–4658. https://doi.org/10.1002/2016gl068949

Ghude, S. D., Fadnavis, S., Beig, G., Polade, S. D., & van der A, R. J. (2008). Detection of surface emission hot spots, trends, and seasonal cycle from satellite-retrieved NO_2 over India. *Journal of Geophysical Research*, *113*, D20305. https://doi.org/10.1029/2007JD009615

Giglio, L., Justice, C. (2015). MOD14A2 MODIS*/Terra thermal anomalies/fire 8-day L3 global 1 km SIN grid V006* [data set]. NASA EOSDIS LP DAAC. https://doi.org/10.5067/MODIS/MOD14A2.006

Girolamo, L. D., Bond, T. C., Bramer, D., Diner, D. J., Fettinger, F., Kahn, R. A., et al. (2004). Analysis of Multi-angle Imaging SpectroRadiometer (MISR) aerosol optical depths over greater India during winter 2001–2004. *Geophysical Research Letters*, *31*, L23115. https://doi.org/10.1029/2004GL021273

Global Modeling and Assimilation Office (2015). MERRA-2 tavgM_2d_aer_Nx: 2d,Monthly mean, Time-averaged, Single-Level, Assimilation, Aerosol Diagnostics V5.12.4, Greenbelt, MD, USA, Goddard Earth Sciences Data and Information Services Center (GES DISC), Accessed [2018]. 10.5067/FH9A0MLJPC7N

Gurjar, B., Jain, A., Sharma, A., Agarwal, A., Gupta, P., Nagpure, A., & Lelieveld, J. (2010). Human health risks in megacities due to air pollution. *Atmospheric Environment*, *44*(36), 4606–4613. https://doi.org/10.1016/j.atmosenv.2010.08.011

Gustafsson, O., Krusa, M., Zencak, Z., Sheesley, R. J., Granat, L., Engstrom, E., & Rodhe, H. (2009). Brown clouds over South Asia: Biomass or fossil fuel combustion? *Science*, *323*(5913), 495–498. https://doi.org/10.1126/science.1164857

Guttikunda, S. K., Goel, R., & Pant, P. (2014). Nature of air pollution, emission sources, and management in the Indian cities. *Atmospheric Environment*, *95*, 501–510. https://doi.org/10.1016/j.atmosenv.2014.07.006

Guttikunda, S. K., & Jawahar, P. (2012). Application of SIM-air modeling tools to assess air quality in Indian cities. *Atmospheric Environment*, *62*, 551–561. https://doi.org/10.1016/j.atmosenv.2012.08.074

Hirsch, R. M., & Slack, J. R. (1984). A nonparametric trend test for seasonal data with serial dependence. *Water Resources Research*, *20*, 727–732. https://doi.org/10.1029/WR020i006p00727

Holben, B. N., Tanré, D., Smirnov, A., Eck, T. F., Slutsker, I., Abuhassan, N., et al. (2001). An emerging ground-based aerosol climatology: Aerosol optical depth from AERONET. *Journal of Geophysical Research*, *106*, 12,067–12,097. https://doi.org/10.1029/2001JD900014

Jain, N., Bhatia, A., & Pathak, H. (2014). Emission of air pollutants from CRB in India. *Aerosol and Air Quality Research*, *14*(1), 422–430.

Janssen, N. (2012). Health effects of black carbon. World Health Organization, Regional Office for Europe.

Kaskaoutis, D. G., Kumar, S., Sharma, D., Singh, R. P., Kharol, S. K., Sharma, M., et al. (2014). Effects of CRB on aerosol properties, plume characteristics, and long-range transport over northern India. *Journal of Geophysical Research: Atmospheres*, *119*, 5424–5444. https://doi.org/10.1002/2013jd021357

Kedia, S., Ramachandran, S., Holben, B., & Tripathi, S. (2014). Quantification of aerosol type, and sources of aerosols over the Indo-Gangetic Plain. *Atmospheric Environment*, *98*, 607–619. https://doi.org/10.1016/j.atmosenv.2014.09.022

Kumar, K. R., Narasimhulu, K., Balakrishnaiah, G., Reddy, B. S. K., Gopal, K. R., Reddy, R. R., et al. (2011). Characterization of aerosol black carbon over a tropical semi-arid region of Anantapur, India. *Atmospheric Research*, *100*(1), 12–27. https://doi.org/10.1016/j.atmosres.2010.12.009

Kumar, P., Kumar, S., & Joshi, L. (2014). Problem of residue management due to rice wheat crop rotation in Punjab. *Socioeconomic and Environmental Implications of Agricultural Residue Burning Springer Briefs in Environmental Science*, 1–12. https://doi.org/10.1007/978-81-322-2014-5_1

Kumar, R., Barth, M. C., Pfister, G. G., Nair, V. S., Ghude, S. D., & Ojha, N. (2015). What controls the seasonal cycle of black carbon aerosols in India? *Journal of Geophysical Research: Atmospheres*, *120*, 7788–7812. https://doi.org/10.1002/2015jd023298

Labonne, M., Bréon, F., & Chevallier, F. (2007). Injection height of biomass burning aerosols as seen from a spaceborne lidar. *Geophysical Research Letters*, *34*, L11806. https://doi.org/10.1029/2007GL029311

Laumbach, R. J., & Kipen, H. M. (2012). Respiratory health effects of air pollution: Update on biomass smoke and traffic pollution. *Journal of Allergy and Clinical Immunology*, *129*(1), 3–11. https://doi.org/10.1016/j.jaci. 2011.11.021

Liu, T., Marlier, M. E., Defries, R. S., Westervelt, D. M., Xia, K. R., Fiore, A. M., et al. (2018). Seasonal impact of regional outdoor biomass burning on air pollution in three Indian cities: Delhi, Bengaluru, and Pune. *Atmospheric Environment*, *172*, 83–92. https://doi.org/10.1016/j.atmosenv.2017.10.024

Manjunatha, K., Shirwal, S., Sushilendra, V. P., & Raghavendra, V. (2015). Role of Balers in agricultural crop residue management-A review.

Mann, H. B. (1945). Nonparametric tests against trend. *Econometrica*, *13*(3), 245. https://doi.org/10.2307/1907187

Meehl, G. A., Arblaster, J. M., & Collins, W. D. (2008). Effects of black carbon aerosols on the Indian monsoon. *Journal of Climate*, *21*(12), 2869–2882. https://doi.org/10.1175/2007jcli1777.1

Menon, S. (2002). Climate effects of black carbon aerosols in China and India. *Science*, *297*(5590), 2250–2253. https://doi.org/10.1126/science.1075159

Moorthy, K. K., Babu, S. S., Manoj, M. R., & Satheesh, S. K. (2013). Buildup of aerosols over the Indian region. *Geophysical Research Letters*, *40*, 1011–1014. https://doi.org/10.1002/grl.50165

Nair, V. S., Moorthy, K. K., Alappattu, D. P., Kunhikrishnan, P. K., George, S., Nair, P. R., et al. (2007). Wintertime aerosol characteristics over the Indo-Gangetic Plain (IGP): Impacts of local boundary layer processes and long-range transport. *Journal of Geophysical Research*, *112*, D13205. https://doi.org/10.1029/2006JD008099

O'neill, N. T. (2003). Spectral discrimination of coarse and fine mode optical depth. *Journal of Geophysical Research*, *108*(D17), 4559. https://doi.org/10.1029/2002JD002975

Pandey, S. K., Vinoj, V., Landu, K., & Babu, S. S. (2017). Declining pre-monsoon dust loading over South Asia: Signature of a changing regional climate. *Scientific Reports*, *7*(1), 16062. https://doi.org/10.1038/s41598-017-16338-w

Patil, M., Patil, S., Waghmare, R., & Dharmaraj, T. (2013). Planetary boundary layer height over the Indian subcontinent during extreme monsoon years. *Journal of Atmospheric and Solar-Terrestrial Physics*, *92*, 94–99. https://doi.org/10.1016/j.jastp.2012.10.011

Prasad, A. K., Singh, R. P., & Singh, A. (2006). Seasonal climatology of aerosol optical depth over the Indian subcontinent: Trend and departures in recent years. *International Journal of Remote Sensing*, *27*(12), 2323–2329. https://doi.org/10.1080/01431160500043665

Pucher, J., Korattyswaropam, N., Mittal, N., & Ittyerah, N. (2005). Urban transport crisis in India. *Transport Policy*, *12*(3), 185–198. https://doi.org/10.1016/j.tranpol.2005.02.008

Ram, K., Sarin, M. M., & Hegde, P. (2010). Long-term record of aerosol optical properties and chemical composition from a high-altitude site (Manora peak) in central Himalaya. *Atmospheric Chemistry and Physics*, *10*(23), 11,791–11,803. https://doi.org/10.5194/acp-10-11791-2010

Ram, K., Sarin, M. M., & Tripathi, S. N. (2012). Temporal trends in atmospheric PM2.5, PM10, elemental carbon, organic carbon, water-soluble organic carbon, and optical properties: Impact of biomass burning emissions in the Indo-Gangetic Plain. *Environmental Science & Technology*, *46*(2), 686–695. https://doi.org/10.1021/es202857w

Ramachandran, S., & Rajesh, T. A. (2007). Black carbon aerosol mass concentrations over Ahmedabad, an urban location in western India: Comparison with urban sites in Asia, Europe, Canada, and the United States. *Journal of Geophysical Research*, *112*, D06211. https://doi.org/10.1029/2006JD007488

Ramanathan, V. (2007). Role of black carbon in global and regional climate change. In *Testimonial to the House Committee on Oversight and Government Reform*, October 18, 2007.

Ramanathan, V., & Carmichael, G. (2008). Global and regional climate changes due to black carbon. *Nature Geoscience*, *1*(4), 221–227. https://doi.org/10.1038/ngeo156

Rhodes, A. H., Carlin, A., & Semple, K. T. (2008). Impact of black carbon in the extraction and mineralization of phenanthrene in soil. *Environmental Science & Technology*, *42*(3), 740–745. https://doi.org/10.1021/es071451n

Safai, P., Kewat, S., Praveen, P., Rao, P., Momin, G., Ali, K., & Devara, P. (2007). Seasonal variation of black carbon aerosols over a tropical urban city of Pune, India. *Atmospheric Environment*, *41*(13), 2699–2709. https://doi.org/10.1016/j.atmosenv.2006.11.044

Safai, P., Raju, M., Budhavant, K., Rao, P., & Devara, P. (2013). Long term studies on characteristics of black carbon aerosols over a tropical urban station Pune, India. *Atmospheric Research*, *132-133*, 173–184. https://doi.org/10.1016/j.atmosres. 2013.05.002

Safai, P., Raju, M., Maheshkumar, R., Kulkarni, J., Rao, P., & Devara, P. (2012). Vertical profiles of black carbon aerosols over the urban locations in South India. *Science of the Total Environment*, *431*, 323–331. https://doi.org/10.1016/j.scitotenv.2012.05.058

Sarkar, C., Kumar, V., & Vinayak, S. (2013). Massive emissions of carcinogenic benzenoids from paddy residue burning in North India. *Current Science*, 1703–1709.

Sarkar, S. (2017). Phenology and carbon fixing: A satellite-based study over continental USA. *International Journal of Remote Sensing*, *39*(1), 1–16. https://doi.org/10.1080/01431161.2017.1378457

Sarkar, S., Chokngamwong, R., Cervone, G., Singh, R., & Kafatos, M. (2006). Variability of aerosol optical depth and aerosol forcing over India. *Advances in Space Research*, *37*(12), 2153–2159. https://doi.org/10.1016/j.asr.2005.09.043

Satheesh, S. K., Babu, S. S., Padmakumari, B., Pandithurai, G., & Soni, V. K. (2017). Variability of atmospheric aerosols over India. In *observed climate variability and change over the Indian region* (pp. 221–248). Singapore: Springer. https://doi.org/10.1007/978-981-10-2531-0_13

Sen, P. K. (1968). Estimates of the regression coefficient based on Kendall's tau. *Journal of the American Statistical Association*, *63*(324), 1379–1389. https://doi.org/10.1080/01621459.1968.10480934

Sharma, M., & Maloo, S. (2005). Assessment of ambient air PM and PM and characterization of PM in the city of Kanpur, India. *Atmospheric Environment*, *39*(33), 6015–6026. https://doi.org/10.1016/j.atmosenv.2005.04.041

Sharma, M., Pandey, R., Maheshwary, M., Sengupta, B., Shukla, B. P., & Mishra, A. (2003). Air quality index and its interpretation for the city of Delhi. *Clean Air: International Journal on Energy for a Clean Environment*, *4*(3), 269–283. https://doi.org/10.1615/interjenercleanenv.v4.i3.50

Sharma, S. N., & Prasad, R. (2008). Effect of crop-residue management on the production and agronomic nitrogen efficiency in a rice–wheat cropping system. *Journal of Plant Nutrition and Soil Science*, *171*(2), 295–302. https://doi.org/10.1002/jpln.200700144

Simon, N. B., Alberini, A., Sharma, P. K., & Cropper, M. L. (1998). The health effects of air pollution in Delhi, India. Banco Mundial.

Singh, R. P., Dey, S., Tripathi, S. N., Tare, V., & Holben, B. (2004). Variability of aerosol parameters over Kanpur, northern India. *Journal of Geophysical Research*, *109*, D23206. https://doi.org/10.1029/2004JD004966

Singh, R. P., & Kaskaoutis, D. G. (2014). CRB: A threat to South Asian air quality. *Eos, Transactions American Geophysical Union*, *95*(37), 333–334. https://doi.org/10.1002/2014eo370001

Sreekanth, V., Niranjan, K., & Madhavan, B. L. (2007). Radiative forcing of black carbon over eastern India. *Geophysical Research Letters*, *34*, L17818. https://doi.org/10.1029/2007GL030377

Stein-Zweers, D & Veefkind, P. (2012). OMI/Aura multi-wavelength aerosol optical depth and single scattering albedo L3 1 day best pixel in 0.25 degree × 0.25 degree V3, NASA Goddard Space Flight Center, Goddard Earth Sciences Data and Information Services Center (GES DISC), Accessed [2018]. https://doi.org/10.5067/Aura/OMI/DATA%3004

Times, M. V. (2017). NASA images show CRB surged before toxic smog hit Delhi-NCR. Retrieved from https://www.hindustantimes.com/environment/crop-burning-surged-before-pollution-peaked-in-delhi-ncr-experts/story-J8mwdFWf9CEOF7MvvPcAyN.html

Torres, O. O. (2008). OMI/Aura near UV aerosol optical depth and single scattering albedo L3 1 day 1.0 degree × 1.0 degree V3, NASA Goddard Space Flight Center, Goddard Earth Sciences Data and Information Services Center (GES DISC), Accessed [2018]. https://doi.org/10.5067/Aura/OMI/DATA%3003

Urmila (2017). Crop burning against the environment. *International Journal of Humanities and Social Science Research*, *3*(8), 16–19.

Van Der Werf, G. R., Randerson, J. T., Giglio, L., Van Leeuwen, T. T., Chen, Y., Rogers, B. M., et al. (2017). Global fire emissions estimates during 1997–2016. *Earth System Science Data*, *9*(2), 697.

Vaughan, M. A., Powell, K. A., Winker, D. M., Hostetler, C. A., Kuehn, R. E., Hunt, W. H., et al. (2009). Fully automated detection of cloud and aerosol layers in the CALIPSO lidar measurements. *Journal of Atmospheric and Oceanic Technology*, *26*(10), 2034–2050. https://doi.org/10.1175/2009jtecha1228.1

Vijayakumar, K., Safai, P., Devara, P., Rao, S. V., & Jayasankar, C. (2016). Effects of agriculture CRB on aerosol properties and long-range transport over northern India: A study using satellite data and model simulations. *Atmospheric Research*, *178-179*, 155–163. https://doi.org/10.1016/j.atmosres.2016.04.003

Wang, C. (2007). Impact of direct radiative forcing of black carbon aerosols on tropical convective precipitation. *Geophysical Research Letters*, *34*, L05709. https://doi.org/10.1029/2006GL028416

World Health Organization (2016). World Health Organization ambient air pollution: A global assessment of exposure and burden of disease.